Available online at www.sciencedirect.com

ScienceDirect

Mendeleev Commun., 2024, **34**, 762–765

Mendeleev Communications

Thermodynamics of the formation of polyynes and aromatic species from methane and acetylene

Emmanuel Busillo,*[a] Pavel A. Vlasov,[b] Valery I. Savchenko,[c] Vladimir N. Smirnov[b] and Vladimir S. Arutyunov[a,b,c]

[a] *National University of Oil and Gas 'Gubkin University', 119991 Moscow, Russian Federation. E-mail: emmanuel.busillo@gmail.com*

[b] *N. N. Semenov Federal Research Center for Chemical Physics, Russian Academy of Sciences, 119991 Moscow, Russian Federation*

[c] *Federal Research Center of Problems of Chemical Physics and Medicinal Chemistry, Russian Academy of Sciences, 142432 Chernogolovka, Moscow Region, Russian Federation*

DOI: 10.1016/j.mencom.2024.09.044

The Gibbs free energies of the formation of several polyynes (C_6H_2, $C_{10}H_2$ and $C_{16}H_2$) and aromatic species (C_6H_6, $C_{10}H_8$ and $C_{16}H_{10}$) from methane and acetylene at temperatures of 1000–2600 K and atmospheric pressure were obtained by quantum chemical calculations using the RI-MP2 method in the ORCA open source software. At lower temperatures, aromatic species form more readily than polyynes, while at temperatures >2200 K the trend reverses and polyyne formation becomes predominant.

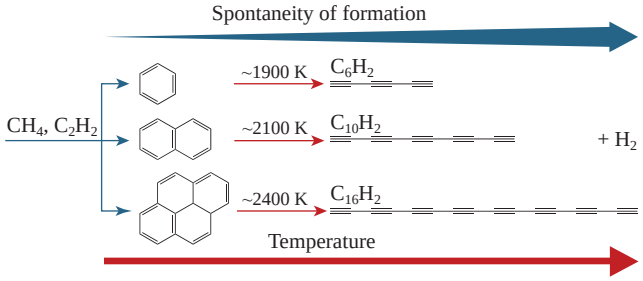

Keywords: acetylene, methane, aromatic compounds, polyynes, quantum chemical calculations, thermodynamic analysis.

Soot particles are the result of incomplete combustion of carbon-containing fuels and pose serious problems to both environmental quality and human health.[1] Despite the great development and success in the study of various processes of combustion and pyrolysis of a number of hydrocarbons,[2–4] our understanding of the intricate mechanisms of formation and growth of soot particles remains incomplete. In particular, soot inception is regarded as one of the most discussed steps in soot formation.[5] In fact, it is generally accepted that soot formation is mainly the result of dimerization processes of grown polyaromatic hydrocarbons (PAHs).[6] However, some discrepancies between this inception pathway and experiments have been found in the literature. First of all, the fact that the forces regarded responsible for the formation of dimers (*i.e.*, van der Waals type) are intrinsically weak under known conditions of soot formation, where the temperature is very high and the characteristic lifetimes of dimers are insufficient to allow nucleation to occur.[7] Furthermore, the growth of large PAHs seems to take place after the formation of soot particles.[8] The growth of PAHs appears to be slower than the more probable polymerization processes.[9] In addition, during the pyrolysis of acetylene, soot is formed even at those temperatures at which thermal destruction of aromatic compounds is expected. As a result, several pathways for the inception and nucleation of soot have been proposed.[10,11] One of these alternative routes involves the formation and polymerization of polyacetylene species with alternating triple and single C–C bonds, *i.e.*, polyynes.[12,13] Polyynes have been experimentally detected in the soot zone of flames of a number of fuel-rich mixtures with components such as C_2H_2, C_2H_4, C_3H_8, C_6H_6 and C_2H_5OH.[14,15] Polyynes arise very fast in these systems, they are present in considerable concentrations, and their cyclization and/or growth is thought to be responsible for the formation of soot nuclei.

In light of these considerations, this work aims to provide a preliminary thermodynamic analysis of the stability and tendency to form such polyacetylene species from methane and acetylene, providing comparison with aromatic molecules based on the same number of carbon atoms. C_6H_2, $C_{10}H_2$ and $C_{16}H_2$ were qualitatively compared with their aromatic analogs C_6H_6, $C_{10}H_8$ and $C_{16}H_{10}$. The Gibbs free energy changes under different conditions were obtained from quantum chemical calculations based on the Møller–Plesset second-order perturbation method with the identity solution (RI-MP2[16]) included in the ORCA software.[17]

The RI-MP2 method is a valuable computational technique in quantum chemistry that has several advantages such as efficiency and speed, accuracy and scalability. It significantly reduces the computational cost and time required for electron correlation calculations compared to traditional MP2 methods. This is achieved by approximating electron repulsion integrals using a resolution of identity, which simplifies the computation without significantly sacrificing accuracy. In practice, an RI-MP2 energy calculation requires an order of magnitude less computational cost than the comparable MP2 calculation. What is more, RI-MP2 scales better than conventional MP2 with the size of the molecular system: this makes it more feasible for larger systems that would otherwise be computationally prohibitive within standard MP2.

The basis set chosen for the simulations is the Dunning correlation-consistent (triple zeta) basis set, cc-pVTZ, which is intended to systematically reduce calculations to the full basis set limit using empirical extrapolation methods.[18] Firstly, the structures of the species treated in this work were optimized using geometry optimization calculations. In ORCA, the default method used for molecular geometry optimization relies on gradient-based techniques and the optimization is performed in redundant internal coordinates. Due to the balance between computational

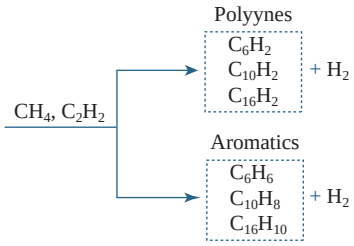

Scheme 1 Formation of polyynes and aromatics from methane and acetylene.

efficiency and convergence reliability, a variant of the quasi-Newton method, the Broyden–Fletcher–Goldfarb–Shanno algorithm, is used as the default choice. It approximates the Hessian matrix from previous gradient evaluations, which helps guide optimization steps to the minimum energy configuration without the need to explicitly calculate second derivatives: this makes it faster and less memory-intensive than methods that require full Hessian evaluation.

After optimization, vibrational analysis is performed using the same level of theory and basis set to ensure consistency. This step is crucial because it not only confirms whether the resulting structure is a minimum (no imaginary frequencies), but also provides the data needed to calculate the thermodynamic properties. The zero point energy (ZPE), *i.e.*, the energy contribution arising from quantum mechanical motion at 0 K, is then calculated based on the vibrational frequencies obtained in the previous step. In addition, thermal corrections to energy, enthalpy and entropy at a given temperature are calculated using the vibrational, rotational and translational modes of the molecule. These corrections account for the temperature-dependent changes in these molecular motions. As a result, Gibbs free energy values were calculated from knowledge of the enthalpy and entropy terms, the former being regarded as the sum of the internal energy at 0 K (including ZPE) plus thermal corrections for enthalpy at the desired temperature, and the latter obtained considering the contributions of molecular motions (translational, rotational and vibrational) at a specific temperature.

The change in the Gibbs free energy for the reactions of the formation of polyynes and aromatic species from CH_4 and C_2H_2 in the temperature range 1000–2600 K at atmospheric pressure was calculated by considering the following reactions (Scheme 1):

$$a\mathrm{CH_4} = \text{polyyne/aromatic species} + b\mathrm{H_2}, \quad (1)$$

$$a'\mathrm{C_2H_2} = \text{polyyne/aromatic species} + b'\mathrm{H_2}, \quad (2)$$

where a, b and a', b' are the stoichiometric coefficients that balance the formation of a particular polyyne and aromatic molecule.

Changes in the Gibbs free energy for the reactions of the formation of polyynes and aromatic hydrocarbons from methane and acetylene are graphically depicted in Figures 1 and 2.

$$6\mathrm{CH_4} \rightarrow \mathrm{C_6H_6} + 9\mathrm{H_2} \quad (3)$$

$$6\mathrm{CH_4} \rightarrow \mathrm{C_6H_2} + 11\mathrm{H_2} \quad (4)$$

$$10\mathrm{CH_4} \rightarrow \mathrm{C_{10}H_8} + 16\mathrm{H_2} \quad (5)$$

$$10\mathrm{CH_4} \rightarrow \mathrm{C_{10}H_2} + 19\mathrm{H_2} \quad (6)$$

$$16\mathrm{CH_4} \rightarrow \mathrm{C_{16}H_{10}} + 27\mathrm{H_2} \quad (7)$$

$$16\mathrm{CH_4} \rightarrow \mathrm{C_{16}H_2} + 31\mathrm{H_2} \quad (8)$$

$$3\mathrm{C_2H_2} \rightarrow \mathrm{C_6H_6} \quad (9)$$

$$3\mathrm{C_2H_2} \rightarrow \mathrm{C_6H_2} + 2\mathrm{H_2} \quad (10)$$

$$5\mathrm{C_2H_2} \rightarrow \mathrm{C_{10}H_8} + \mathrm{H_2} \quad (11)$$

$$5\mathrm{C_2H_2} \rightarrow \mathrm{C_{10}H_2} + 4\mathrm{H_2} \quad (12)$$

$$8\mathrm{C_2H_2} \rightarrow \mathrm{C_{16}H_{10}} + 3\mathrm{H_2} \quad (13)$$

$$8\mathrm{C_2H_2} \rightarrow \mathrm{C_{16}H_2} + 7\mathrm{H_2} \quad (14)$$

As can be seen from Figure 1, at relatively low temperatures, *i.e.*, $T < 1800$ K, the formation reactions of aromatic hydrocarbons have lower ΔG values than the reactions of polyyne formation.

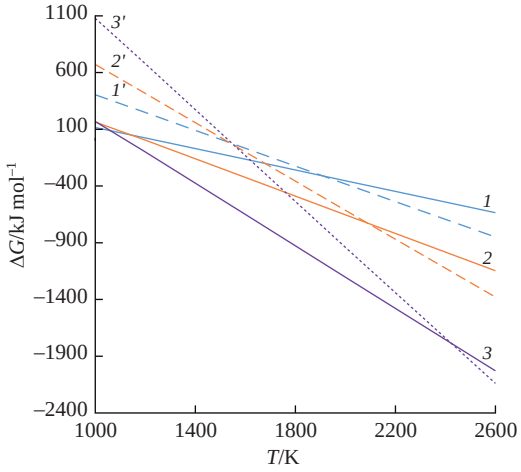

Figure 1 Changes in Gibbs free energy for reactions of methane conversion into products (*1*) C_6H_6, (*1′*) C_6H_2, (*2*) $C_{10}H_8$, (*2′*) $C_{10}H_2$, (*3*) $C_{16}H_{10}$ and (*3′*) $C_{16}H_2$ [reactions (3)–(8)] at different temperatures in the range of 1000–2600 K and atmospheric pressure.

It is known that at 1300 K, benzene is thermodynamically more stable than methane, and the stability of aromatic compounds as a function of temperature increases faster than that of olefins.[19] However, at high temperatures, both C–C and C–H bonds are broken and triple bond formation becomes possible.[19] An increase in temperature causes a change in the trends observed in Figure 1: the ΔG for the formation of polyynes becomes less than the ΔG for the formation of aromatic molecules with the same number of carbon atoms. In particular, the intersection points of the graphs of temperature dependences of ΔG values for the formation reactions of aromatic hydrocarbons and polyynes are at ~1900, ~2100 and ~2400 K for C_6H_6 *vs.* C_6H_2, $C_{10}H_8$ *vs.* $C_{10}H_2$ and $C_{16}H_{10}$ *vs.* $C_{16}H_2$, respectively.

These considerations are consistent with other experimental and theoretical studies supporting that the most stable structures of carbon clusters up to C_{20} are chains and monocycles.[20] The results obtained are very similar to those[12] regarding the formation of short polyynes and aromatics from graphite and molecular hydrogen: in this case, the intersection points of the ΔG *vs.* T graphs for the reactions of the formation of aromatic hydrocarbons and polyynes were observed at ~1700, ~1825 and ~2100 K for benzene, naphthalene and pyrene, respectively.

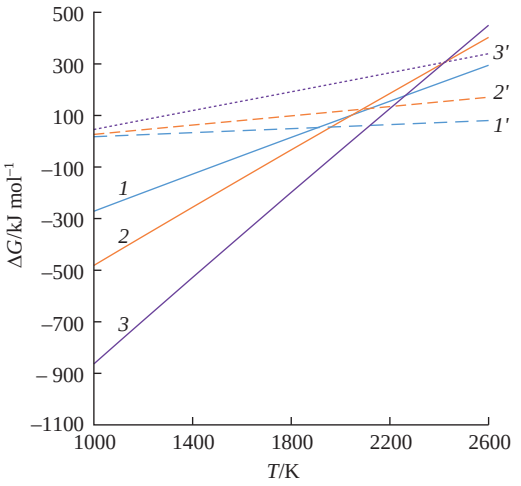

Figure 2 Changes in Gibbs free energy for reactions of acetylene conversion into products (*1*) C_6H_6, (*1′*) C_6H_2, (*2*) $C_{10}H_8$, (*2′*) $C_{10}H_2$, (*3*) $C_{16}H_{10}$ and (*3′*) $C_{16}H_2$ [reactions (9)–(14)] at different temperatures in the range of 1000–2600 K and atmospheric pressure.

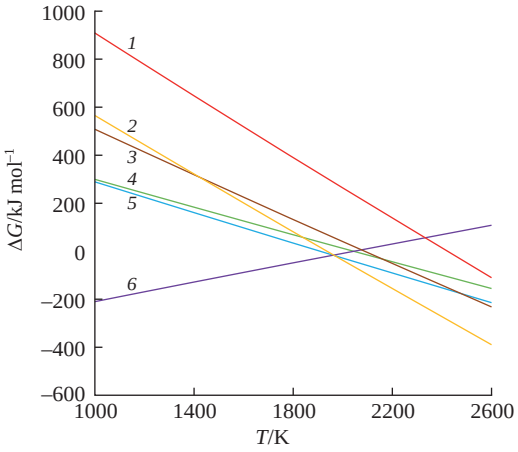

Figure 3 Changes in Gibbs free energy for the reactions of conversion of aromatic compounds into polyynes (*1*) $C_{16}H_2$, (*2*) $C_{12}H_2$, (*3*) $C_{10}H_2$, (*4*) C_8H_2 and (*5*) C_6H_2 [reactions (15)–(19)] at different temperatures in the range of 1000–2600 K and atmospheric pressure compared to the reaction of formation of (*6*) naphthalene from benzene and acetylene [reaction (20)].

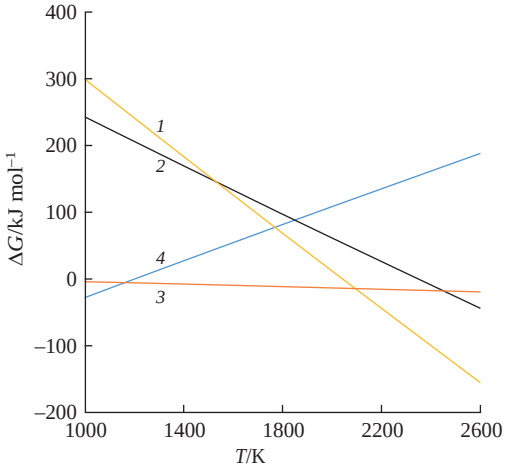

Figure 4 Changes in Gibbs free energy for the reactions of benzene and acetylene to form various unsaturated hydrocarbons (*1*) C_8H_2, (*2*) C_8H_4, (*3*) C_8H_6 and (*4*) C_8H_8 [reactions (21)–(24)] at different temperatures in the range of 1000–2600 K and atmospheric pressure.

In Figure 2, the observed trend is consistent with that observed previously, except that with increasing temperature, acetylene consumption (regardless of the species formed) shows an increase in the change in Gibbs free energy, assuming more and more positive values, thereby indicating a higher probability of reverse reactions, *i.e.*, formation of acetylene. From a thermodynamic point of view, acetylene plays a predominant role in the temperature range $1473 < T < 2500$ K:[19] at high temperatures it is more stable than benzene,[19] and, together with polyynes, persists in the gas phase as the most stable structures.[12]

To compare the probability of formation of aromatic compounds and polyynes, we plotted the temperature dependences of the changes in Gibbs free energy for several hypothetic reactions of the conversion of aromatic compounds into polyynes (Figure 3):

$$C_{16}H_{10} \rightarrow C_{16}H_2 + 4H_2, \quad (15)$$
$$2C_6H_6 \rightarrow C_{12}H_2 + 5H_2, \quad (16)$$
$$C_{10}H_8 \rightarrow C_{10}H_2 + 3H_2, \quad (17)$$
$$C_6H_6 + C_2H_2 \rightarrow C_8H_2 + 3H_2, \quad (18)$$
$$C_6H_6 \rightarrow C_6H_2 + 2H_2. \quad (19)$$

With increasing temperature, the change in Gibbs free energy decreases for all reactions involved in the consumption of aromatic compounds and the formation of polyynes. For comparison, Figure 3 also shows the oppositely directed reaction of the formation of naphthalene from benzene and acetylene, in which Gibbs free energy increases with temperature:

$$C_6H_6 + 2C_2H_2 \rightarrow C_{10}H_8 + H_2. \quad (20)$$

The evolution of the temperature dependence of changes in the Gibbs free energy for reactions of the transformation of aromatic compounds into hydrocarbons with different degrees of unsaturation is shown by the example of a series of reactions (Figure 4):

$$C_6H_6 + C_2H_2 \rightarrow C_8H_2 + 3H_2, \quad (21)$$
$$C_6H_6 + C_2H_2 \rightarrow C_8H_4 + 2H_2, \quad (22)$$
$$C_6H_6 + C_2H_2 \rightarrow C_8H_6 + H_2, \quad (23)$$
$$C_6H_6 + C_2H_2 \rightarrow C_8H_8. \quad (24)$$

It is clearly seen that with increasing temperature, the probability of the formation of unsaturated hydrocarbons, including polyynes, increases. This is a concequence of the release of more H_2 molecules, which leads to an increase in entropy due to the increase in the number of molecules in the gas phase.[21] This is also valid for methane conversion [Figure S1(*a*), see Online Supplementary Materials], where the stoichiometry of reactions is related to an increase in the number of moles of products. However, when it comes to acetylene conversion [Figure S2(*b*)], the situation changes, *i.e.*, the stoichiometry of reactions leads to a decrease or absence of a net change in the number of moles between reactants and products and a decrease in entropy is observed. It is important to note that changes in entropy are determined not only by the number of molecules in the gas phase; changes in molecular complexity and energy distribution between products and reactants may also be responsible for significant changes.

In conclusion, this article presents the results of quantum chemical simulations of changes in the Gibbs free energy for the formation reactions of a number of polyynes and aromatic compounds using methane and acetylene as reactants in the temperature range of 1000–2600 K at atmospheric pressure. It has been found that at relatively low temperatures (1000–1900 K) the probability of the formation of aromatic species is higher than that of polyynes. However, at higher temperatures ($T > 1900$ K), the trend is reversed, as the thermodynamic stability of polyynes becomes higher.

The results obtained confirm the possibility of a significant contribution of the polyyne mechanism at the initial stage of soot nucleation, at least during the pyrolysis of acetylene and methane at high temperatures. However, the role of the polyyne mechanism can be further clarified by complementing the above thermodynamics analysis by kinetic simulations.

Online Supplementary Materials

Supplementary data associated with this article can be found in the online version at doi: 10.1016/j.mencom.2024.09.044.

References

1 B. S. Haynes and H. Gg. Wagner, *Prog. Energy Combust. Sci.*, 1981, **7**, 229.
2 E. Ranzi, M. Dente, A. Goldaniga, G. Bozzano and T. Faravelli, *Prog. Energy Combust. Sci.*, 2001, **27**, 99.
3 G. L. Agafonov, I. V. Bilera, P. A. Vlasov, I. V. Zhil'tsova, Yu. A. Kolbanovskii, V. N. Smirnov and A. M. Tereza, *Kinet. Catal.*, 2016, **57**, 557 (*Kinet. Katal.*, 2016, **57**, 571).
4 I. A. Makaryan, E. A. Salgansky, V. S. Arutyunov and I. V. Sedov, *Energies*, 2023, **16**, 2916.
5 R. M. Mironenko, V. A. Likholobov and O. B. Belskaya, *Russ. Chem. Rev.*, 2022, **91**, RCR5017.
6 M. Frenklach and H. Wang, *Symp. (Int.) Combust., [Proc.]*, 1991, **23**, 1559.
7 H. Sabbah, L. Biennier, S. J. Klippenstein, I. R. Sims and B. R. Rowe, *J. Phys. Chem. Lett.*, 2010, **1**, 2962.

8 K. Siegmann, K. Sattler and H. C. Siegmann, *J. Electron Spectrosc. Relat. Phenom.*, 2002, **126**, 191.
9 P. Minutolo, G. Gambi, A. D'Alessio and A. D'Anna, *Combust. Sci. Technol.*, 1994, **101**, 311.
10 J. W. Martin, M. Salamanca and M. Kraft, *Prog. Energy Combust. Sci.*, 2022, **88**, 100956.
11 E. Busillo, P. Vlasov and V. Arutyunov, *Mendeleev Commun.*, 2022, **32**, 700.
12 A. V. Krestinin, *Symp. (Int.) Combust., [Proc.]*, 1998, **27**, 1557.
13 A. V. Krestinin, *Combust. Flame*, 2000, **121**, 513.
14 U. Bonne, K. H. Homann and H. Gg. Wagner, *Symp. (Int.) Combust., [Proc.]*, 1965, **10**, 503.
15 K. H. Homann and H. Gg. Wagner, *Symp. (Int.) Combust., [Proc.]*, 1967, **11**, 371.
16 M. Feyereisen, G. Fitzgerald and A. Komornicki, *Chem. Phys. Lett.*, 1993, **208**, 359.
17 F. Neese, F. Wennmohs, U. Becker and C. Riplinger, *J. Chem. Phys.*, 2020, **152**, 224108.
18 D. E. Woon and T. H. Dunning, Jr., *J. Chem. Phys.*, 1994, **100**, 2975.
19 C. Guéret, M. Daroux and F. Billaud, *Chem. Eng. Sci.*, 1997, **52**, 815.
20 G. von Helden, M. T. Hsu, N. Gotts and M. T. Bowers, *J. Phys. Chem.*, 1993, **97**, 8182.
21 H. Wang, *Proc. Combust. Inst.*, 2011, **33**, 41.

Received: 17th April 2024; Com. 24/7471